

Safety and Biodistribution of Human Bone Marrow-Derived Mesenchymal Stromal Cells Injected Intrathecally in Non-Obese Diabetic Severe Combined Immunodeficiency Mice: Preclinical Study

Mari Paz Quesada¹  · David García-Bernal^{1,2} · Diego Pastor³ · Alicia Estirado⁴ · Miguel Blanquer^{1,2} · Ana M^a García-Hernández¹ · José M. Moraleda^{1,2} · Salvador Martínez^{4,5,6}

Received: 27 May 2019 / Revised: 2 July 2019 / Accepted: 3 July 2019 / Published online: 26 July 2019
© The Korean Tissue Engineering and Regenerative Medicine Society 2019

Abstract

BACKGROUND: Mesenchymal stromal cells (MSCs) have potent immunomodulatory and neuroprotective properties, and have been tested in neurodegenerative diseases resulting in meaningful clinical improvements. Regulatory guidelines specify the need to perform preclinical studies prior any clinical trial, including biodistribution assays and tumourigenesis exclusion. We conducted a preclinical study of human bone marrow MSCs (hBM-MSCs) injected by intrathecal route in Non-Obese Diabetic Severe Combined Immunodeficiency mice, to explore cellular biodistribution and toxicity as a privileged administration method for cell therapy in Friedreich's Ataxia.

METHODS: For this purpose, 3×10^5 cells were injected by intrathecal route in 12 animals (experimental group) and the same volume of culture media in 6 animals (control group). Blood samples were collected at 24 h (n = 9) or 4 months (n = 9) to assess toxicity, and nine organs were harvested for histology and safety studies. Genomic DNA was isolated from all tissues, and mouse GAPDH and human β 2M and β -actin genes were amplified by qPCR to analyze hBM-MSCs biodistribution.

RESULTS: There were no deaths nor acute or chronic toxicity. Hematology, biochemistry and body weight were in the range of normal values in all groups. At 24 h hBM-MSCs were detected in 4/6 spinal cords and 1/6 hearts, and at 4 months in 3/6 hearts and 1/6 brains of transplanted mice. No tumours were found.

CONCLUSION: This study demonstrated that intrathecal injection of hBM-MSCs is safe, non toxic and do not produce tumors. These results provide further evidence that hBM-MSCs might be used in a clinical trial in patients with FRDA.

Keywords Intrathecal transplantation · Bone marrow-derived mesenchymal stromal cells · Friedreich's Ataxia · Neuroprotection · Preclinical study

✉ Mari Paz Quesada
mpquesada@umh.es

¹ Cellular Therapy and Hematopoietic Transplant Unit, Hematology Department, Virgen de la Arrixaca Clinical University Hospital, Biomedical Research Institute of Murcia, IMIB-Arrixaca, Campus of International Excellence "Campus Mare Nostrum" University of Murcia, Carretera Acceso Urbanización Buenavista (1^a izda), 30120 El Palmar, Murcia, Spain

² Internal Medicine Department, Medicine School, University of Murcia, Virgen de la Arrixaca Clinical University Hospital, Ctra. Madrid-Cartagena, s/n, 30120 El Palmar, Murcia, Spain

³ Sport Research Center, University Miguel Hernández of Elche, Av. de la Universidad s/n, 03202 Elche, Alicante, Spain

⁴ Neuroscience Institute UMH-CSIC, University Miguel Hernández of Elche, Carretera de Valencia, Km 18, 03550 San Juan, Alicante, Spain

⁵ CIBERSAM-ISCIH, Avenida Blasco Ibáñez 15, 46010 Valencia, Spain

⁶ Human Anatomy Department, Medicine School, University Miguel Hernández of Elche, Carretera de Valencia, Km 18, 03550 San Juan, Alicante, Spain

1 Introduction

Prior to launch a clinical human trial, regulatory agencies require preclinical data showing the biodistribution, safety and efficacy of the therapeutic agent in animal models. And for the early phases of clinical development, biodistribution studies not reproducing the pathological condition in humans, as Friedreich's Ataxia (FRDA), but using the expected route of administration in immunodeficient animals are accepted [1]. FRDA is an autosomal recessive inherited neurodegenerative disorder caused by a GAA triplet repeat expansion in the first intron of the frataxin (FXN) gene [2], which impedes the total transcription of the gene [3]. As a result, the cells present a deficiency of the FXN protein, which causes numerous alterations in mitochondrial iron metabolism, biosynthesis of the iron-sulphur cluster, as well as in oxidative stress regulation, leading to mitochondrial dysfunction [4]. This pathology is the most prevalent inherited ataxia. It is associated with progressive deterioration and a shortened lifespan (mean 35–40 years) [5, 6] and it is characterized by diverse clinical and progressive neuropathological phenotypes, abnormalities of the heart, skeleton, and pancreas [5, 7–9]. GAA repeat expansion is longer in the heart and pancreas, which could explain the malfunction of these vital organs, leading to hypertrophic cardiomyopathy and diabetes mellitus [10]. In the nervous system, the large sensory neurons of the dorsal root ganglia (DRG) in the spinal cord are especially susceptible, and are progressively destroyed in the presence of inflammation signals, producing sensory neuropathy [4, 9].

Despite the development of new drugs [8], currently there are no effective therapeutic options to halt the progression of sensitive and motor deficiency in FRDA patients, that is an unmet clinical need. Cell therapy with mesenchymal stromal cells (MSCs) has recently emerged as a promising treatment for a wide variety of neurodegenerative diseases, due to its anti-inflammatory, immunomodulatory and reparative/regenerative properties [11–15]. MSCs can be easily isolated from bone marrow, adipose tissue, and dental pulp, among other human tissues [16]. They can expand readily *in vitro* and have the property to differentiate into mesodermal lineages (adipogenic, osteogenic and chondrogenic) [17]. In animal models MSCs display neurotrophic properties mediated by several growth factors; mainly glial-derived neurotrophic factor (GDNF), brain-derived neurotrophic factor (BDNF), neurotrophin-3 (NT3), neurotrophin-4 (NT4), vascular endothelial growth factor (VEGF), as well as immunosuppressive effects by cytokines with paracrine and autocrine actions in the injured tissues. These neurotrophic properties help to modulate favorably the local immune

system, to reduce oxidative stress and apoptosis, and to stimulate angiogenesis and regeneration of local stem cells [14, 18]. MSCs therapies are feasible and safe, and they improve the functional performance in neurodegeneration, both in animal models as well as in several human clinical trials [12, 19, 20]. Therefore, MSCs therapy might be a good candidate to improve the natural history of patients with FRDA.

In our lab, we have described that periodontal ligament stromal cells (PLSCs) proliferate in culture, and after being grafted into the brain, present neural crest stem cells properties [13]. Moreover, in PLSCs isolated from FRDA patients, as a cellular model of this disease, we also have described an altered gene expression related to cell cycle, oxidative stress and iron homeostasis; and we showed changes in miRNA-886-3p and miRNA-132-3p expressions, and hypermethylation of the frataxin gene in the upstream GAA repetitive region [21]. In addition, we showed that adipose stem cell-conditioned medium added to these cells, reduces caspase-3 active levels, increases frataxin protein expression, increases cell survival through different factors, and protects these FRDA-PLSCs from oxidative stress [22, 23]. We also confirmed this effect in the DRGs of FRDA cells isolated from YG8 mice, a model of FRDA, using both bone marrow-conditioned medium from wild-type or from YG8 mice, resulting in an increased of the survival of these degenerated cells [24]. Recently, it has also been seen that FXN and cytochrome-c oxidase subunit 8 (Cox8) mitochondrial proteins are transferred *in vivo* from wild-type mouse hematopoietic stem and progenitor transplanted cells to FRDA mouse neurons and myocytes, thus mediating phenotypic rescue of FRDA in YG8 mice [25].

In other neurodegenerative diseases, our group also demonstrated the neuroprotective capacity of BDNF secreted from bone marrow-derived MSC (BM-MSCs) when they were injected into the hindlimb muscles or into the spinal cord parenchyma of a muscle deficient mice (mdf), a mouse model of motoneuron degeneration [20, 26]. In these works, we were able to show that after infusion of BM-MSCs, neuronal death was reduced, GDNF increased in the spinal cord, and mice motor function significantly improved.

Among the neurological structures affected in FRDA, peripheral sensory neurons of the DRGs are more accessible than central neurons, which are protected by the blood–brain barrier [27]. Hence, in a previous work, we hypothesized that intrathecal injection of BM-MSCs might be a privileged route of cellular infusion to act directly over DRG's neurons, producing neuroprotective and paracrine effects to improve their survival as well as DRG's microenvironment [14]. In this way, we injected intrathecally in FRDA-YG8 mice BM-MSCs isolated from either

wild-type or YG8 mice, showing that both experimental groups presented grafted cells infiltration in the DRGs, improved motor skills, and 5 months after the injection, the number of sensorial neurons and frataxin expression were increased in the DRGs [14]. Therefore, the intrathecal infusion route might be of interest to diminish the neuropathy of FRDA patients and improve their quality of life.

Although in patients with multiple sclerosis it has been demonstrated that intrathecal infusion of MSCs is safe [28], we performed preclinical studies to evaluate not only the safety, but also toxicity and biodistribution of the intrathecal injection of human BM-MSCs (hBM-MSCs) in immunosuppressed Non-Obese Diabetic/Severe Combined Immunodeficiency (NOD/SCID) mice, providing also data of the systemic response. Our results would pave the way for the development of a future clinical trial of intrathecal infusion of hBM-MSCs in patients with FRDA.

2 Materials and methods

2.1 Human BM-MSCs isolation and culture

To isolate hBM-MSCs, bone marrow samples were obtained by percutaneous direct aspiration of bone marrow from the iliac crest of 3 healthy volunteers at Hospital Clínico Universitario Virgen de la Arrixaca (Murcia, Spain). The aspirated bone marrow was transferred to a sterile tube containing sodium heparin (20 U/ml), followed by a Ficoll density gradient-based separation and cell washing using the closed automated SEPAX System (Biosafe, Eysines, Switzerland) to obtain the mononuclear cell fraction. Then, cells were seeded into 75-cm² tissue culture flasks (Corning Costar, Corning, NY, USA) at a density of 1.6×10^5 cells/cm² in Dulbecco's Modified Eagle's-low glucose medium (DMEM, Sigma Aldrich, St. Louis, MO, USA) containing 5% human platelet lysate (hPL), 100 U/ml penicillin (Lonza, Basel, Switzerland), 100 U/ml streptomycin (Lonza, Basel, Switzerland) and 1% L-glutamine (Lonza, Basel, Switzerland) (complete medium), and allowed to attach undisturbed for 2–3 days at 37 °C, 5% CO₂ and 95% humidity. After, non-adherent cells were removed, the flask was rinsed with Ca²⁺/Mg²⁺-free phosphate buffered saline (PBS) (Gibco Invitrogen, Carlsbad, CA, USA), and fresh complete medium was added. When cultures reached 80% of confluence, cells were washed with PBS (Carlsbad, CA, USA) and detached by incubating with Tryple Select dissociation reagent (Gibco, Thermo Fisher Scientific, Waltham, MA, USA) for 5 min at 37 °C and seeded at a density of 5×10^3 cells/cm², replacing medium every 3 days. Human BM-MSCs were then cryopreserved in liquid nitrogen in MSC freezing solution (Biological Industries, Cromwell, CT, USA)

until the experimental procedures. All studies were performed on hBM-MSCs expanded within culture passages 3–4. The use of human bone marrow cells was in accordance with the guidelines and regulations of the Ethics Committee of the Hospital Clínico Universitario Virgen de la Arrixaca (Murcia, Spain). All of the donors provided written informed consent prior to participation in this study.

2.2 Human BM-MSCs immunophenotypic characterization

Expression of mesenchymal stromal cell surface markers was analyzed on cultures of hBM-MSCs by flow cytometry. Briefly, cells were detached, rinsed twice with PBS and incubated in the dark at 4 °C for 30 min with fluorescence-conjugated specific monoclonal antibodies for human CD73, CD90 and CD105; Allophycocyanin (APC, Miltenyi Biotec, Bergisch Gladbach, Germany), Fluorescein isothiocyanate (FITC, Miltenyi Biotec, Bergisch Gladbach, Germany), Phycoerythrin (PE, Miltenyi Biotec, Bergisch Gladbach, Germany) respectively. Lack of expression of the hematopoietic markers CD14, CD20, CD34 and CD45 was also analyzed using Peridinin Chlorophyll-protein complex (PerCP, Miltenyi Biotec, Bergisch Gladbach, Germany). Non-specific fluorescence was measured using specific isotype monoclonal antibodies. Subsequently, cells were acquired using a BD FACS Canto flow cytometer (BD Biosciences, San Jose, CA, USA) and analyzed using Kaluza analysis software (Beckman Coulter, Inc., Brea, CA, USA).

2.3 *In vitro* trilineage mesenchymal differentiation

For multipotent differentiation assays, hBM-MSCs were differentiated toward the adipogenic, osteogenic and chondrogenic mesodermal lineages. Adipogenic differentiation was induced after culturing cells in StemMACS AdipoDiff media (Miltenyi Biotec, Bergisch Gladbach, Germany), following the manufacturer's instructions. After 14 days, cells were fixed in 4% paraformaldehyde (PFA, Sigma Aldrich, St. Louis, MO, USA) and stained with Oil Red O solution (Sigma Aldrich, St. Louis, MO, USA) to detect the accumulation of cytoplasmic lipids droplets. For osteogenic differentiation, hBM-MSCs were cultured in StemMACS OsteoDiff media (Miltenyi Biotec, Bergisch Gladbach, Germany). After 21 days, cells were fixed with 4% PFA (Sigma Aldrich, St. Louis, MO, USA) and stained with Alizarin Red (Sigma Aldrich, St. Louis, MO, USA) to detection of calcium depositions in the cultures. Also, alkaline phosphate activity was assessed by staining with SigmaFast™ BCIP-NBT (Sigma Aldrich, St. Louis, MO, USA). For induction of chondrogenic differentiation, hBM-

MSCs were resuspended at a density of 1×10^6 cells/ml in StemMACS CondroDiff media (Miltenyi Biotec, Bergisch Gladbach, Germany) and cultured at 37 °C and 5% CO₂. After 21 days, cells were fixed in 4% PFA and stained with Alcian blue (Sigma Aldrich, St. Louis, MO, USA) to detect cartilage mucopolysaccharides and glycosaminoglycans.

2.4 NOD/SCID animals

Twelve male and 6 female 9-week old Non-Obese Diabetic Severe Combined Immunodeficiency (NOD/SCID) mice (NOD.CB17-Prkdc^{scid}/NCrHsd) from Envigo (Huntingdon, Cambridgeshire, UK) were used in this study. As preclinical studies require the use of hMSCs in order to be later transferred to clinical studies, we used immunocompromised NOD/SCID rodents to prevent immune rejection of infused human cells, according to the *Laboratory Animal Care guidelines and Good Laboratory Practices (GLP)*. All animals were maintained in a temperature-controlled environment (21 ± 1 °C) with access to food and water ad libitum before and after the experimental procedures, which were adhered to the recommendations of local, national and european laws (Decret 214 of 1997, Real Decret 53 of 2013 and European directive 86/609/EC of 1986, respectively). The procedures performed in this work involving animals were approved by the Ethical Committee on Animal Experimentation at University of Murcia (220/2016). All the experimental procedures involving animals were conducted in accordance with the Institutional Animal care guidelines of Murcia University.

2.5 Human BM-MSCs preparation and mice transplantation

One day before the surgery, one cryotube of hBM-MSCs was quickly thawed and transferred directly into culture cells dishes until next day, moment in which we counted and distributed the cells in 1.5-ml eppendorfs, containing 3×10^5 hBM-MSCs in 5 µl DMEM (Sigma Aldrich, St. Louis, MO, USA) per animal.

Before the transplant, the rodents were treated with analgesia by subcutaneous injection of 0.1 mg/kg buprenorphine (Buprex, Schering-Plough, Madrid, ESP) and 0.1 mg/kg meloxicam (Loxicom, Norbrook, Laboratorios Karizoo, Barcelona, ESP), and 30 min later they were anesthetized with inhaled isoflurane gas (Esteve Veterinary, Milan, ITA). The skin and back muscles between D10-L1 were dissected and spinal cord was exposed by laminectomy. Under a surgical microscope, a Hamilton syringe (Hamilton, Reno, NV, USA) was introduced in the intrathecal space and 3×10^5 hBM-MSCs in 5 µl DMEM (Sigma Aldrich, St. Louis, MO, USA)

(experimental group; n = 12) or 5 µl of DMEM (Sigma Aldrich, St. Louis, MO, USA) (sham/control group; n = 6) were slowly injected in the subarachnoid space reaching the cerebrospinal fluid. After the injection, the incision was sutured and mice were monitored until they recovered from anesthesia, and during the following days, in order to ensure that the operation did not cause any additional motor damage. Afterwards, general condition (food and water intake) and body weight were observed until the end of the experiment.

2.6 Mice tissue collection and histological processing

Twenty-four hours or 4 months after the transplant, mice were anesthetized with isoflurane gas and a blood sample was obtained before they were fixed by intracardiac perfusion of 4% PFA. Blood samples were collected in Ethylenediaminetetraacetic acid (EDTA) potassium tubes to avoid coagulation (Microvette CB 300 K2E, Sarstedt, Barcelona, ESP), and stored at 4 °C during 2 h before they were analyzed. Heart, brain, cerebellum, spinal cord, liver, spleen, lungs, kidneys and gonads from perfused mice were harvested and stored at 4 °C with 4% PFA (Sigma Aldrich, St. Louis, MO, USA) for 24 h. Next, all tissues were dehydrated with alcohol and xylene before they were included in paraffin to be sliced.

For study the possible tumorigenic potential of hBM-MSCs, 12-µm slices paraffin-embedded (FFPE), not serial, from all organs were stained with cresyl-violet (Acros Organics, Thermo Fisher Scientific, Waltham, MA, USA) for histopathological examination using a light field microscope.

2.7 Hematology and plasma biochemistry

Hematological and biochemical parameters were analyzed in blood samples collected from control and experimental mice, at 24 h and 4 months after the transplant. An automatic XN2000 hematology analyzer (Sysmex, Kobe, JPN) was used to measure red blood cell (RBC), hemoglobin (HGB), hematocrit (HCT), mean corpuscular volume (MCV), mean corpuscular hemoglobin (MCH), mean corpuscular hemoglobin concentration (MCHC), platelet, mean platelet volume (MPV), total white blood cell (WBC), neutrophils, lymphocytes, monocytes, eosinophils and basophils. Biochemical data including glucose, urea, total protein (TP), albumin, total bilirubin (TB), Na, K, Cl, triglycerides, total cholesterol (TC), aspartate transaminase (AST) and alanine transaminase (ALT) were measured from plasma in a Cobas 8000 c702 chemistry analyzer (Roche Diagnostics, Basel, CHE).

2.8 Genomic DNA extraction and quantification

Genomic DNA (gDNA) was isolated from the following tissues: heart, gonads, liver, cerebellum, spleen, lungs, spinal cord, brain and kidneys. For this purpose, freshly cut sections of FFPE tissue from each organ were homogenized in a 1.5-ml tube and deparaffinized with 1 ml of xilol. Afterwards, the tissues were processed with the QIAmp DNA FFPE tissue Kit (QIAGEN, Hilden, DEU) according to the manufacturer's instructions. The eluted gDNA concentration was measured and the purity was analyzed in a NanoDrop™ 1000 spectrophotometer system (Thermo Fisher Scientific, Waltham, MA, USA).

2.9 Mouse and human specific real-time PCR primers

To study the presence/absence of the hBM-MSCs injected intrathecally in mice, we amplified the gDNA isolated from all the tissues listed in the previous section by real-time PCR (qPCR). For that we used specific qPCR primers for human β -actin and β 2-microglobulin (β 2M) genes, and for mouse glyceraldehyde-3-phosphate dehydrogenase (GAPDH) gen, which do not amplify crosswise in the other species. For human β -actin, sense-CAAGGGCGCTTCTCTGCAC and antisense-GGATGCCTCTCTTGCTCTGG; for human β 2M sense-GAACATACCTGGGTTGGTTG and antisense-GCCTGGTTAATTTTTGTATTTTCA. And for mouse GAPDH, sense-TTGGGTTGTACATCCAAGCA and antisense-AACCTGCAGCCATCAGCTA.

2.10 Real-time PCR for hBM-MSCs detection and biodistribution study

The real time PCR reactions were done in duplicated with 100 ng of gDNA using SYBR Premix Ex Taq (Takara) following the manufacturer's instructions and ran in the Applied Biosystems StepOnePlus Real-Time PCR System (Thermo Fisher Scientific, Waltham, MA, USA). In each experiment we included one positive mouse and human controls, a negative control without gDNA and a standard curve with mouse and/or human gDNA, with five dilutions points. Both GAPDH and β -actin were amplified in single reactions in the same plate with a hybridization temperature of 64 °C, and therefore with the two standard curves of both species, while β 2M was amplified at 61 °C including only the human standard curve.

In addition to using specific primers, we also included a melting curve with specific melting temperature ($T_m \pm 0.5$ °C) at the end of each qPCR to ensure the precise amplification of our amplicons and no others: GAPDH (80 °C), β -actin (88 °C) and β 2M (85.7 °C). And as quality control, to validate the presence of hBM-MSCs in

any mice tissue, the human DNA (hDNA) amplification must have occurred in both β -actin and β 2M genes. Even more, the amplification of GAPDH as a control in all the tissues will confirm that the reactions ran properly.

2.11 Statistical analysis

Statistical analysis and the significance study between groups were calculated with Sigmaplot v12.0 software, using *t* test. Values were analyzed as mean \pm standard deviation of the mean (SD). *P* values < 0.05 were considered statistically significant.

3 Results

3.1 Isolated hBM-MSCs are positive ($\geq 95\%$) and negative ($\leq 2\%$) for specific MSC surface markers

According to the standard criteria of the International Society for Cellular Therapy (ISCT) [17] to verify the identity of the hBM-MSCs, the cells were seeded in culture flasks under standard conditions and we confirmed that they were adherent to the plastic. Then, we analyzed their specific surface antigen expression by flow cytometry. We observed a high expression pattern levels ($\geq 95\%$) of the mesenchymal markers CD73, CD90 and CD105 and lack expression ($\leq 2\%$) of the hematopoietic markers CD14, CD20, CD34 and CD45 (Fig. 1) which are the first two criteria necessary to be defined as mesenchymal stromal cells.

3.2 Isolated human BM-MSCs are able to differentiate *in vitro* into mesenchymal lineages

To complete the criteria of identification for MSCs, we demonstrated the ability of hBM-MSCs for *in vitro* trilineage mesodermal differentiation (Fig. 2). Differentiation was achieved using commercial and standard *in vitro* culture differentiation conditions as described in the Materials and methods section. Differentiation verification was done by qualitative analysis. Thereby, we identified osteoblasts differentiation using Alizarin Red staining which allows the identification of calcium deposits in the culture with an orange-red color (Fig. 2A); and SigmaFast™ 5-bromo-4-chloro-3-indolyl-phosphate/nitro blue tetrazolium (BCIP-NBT) to assess the alkaline phosphatase (AP) activity. AP is detected using BCIP-NBT as a substrate, which stains the cells in blue-violet when AP is present. Undifferentiated MSCs exhibit weak AP activity, whereas osteoblasts show high AP activity (Fig. 2B). We recognized adipocyte

differentiation using Oil Red O which detects the accumulation of cytoplasmic lipids droplets (Fig. 2C). And finally, chondroblasts were identified with Alcian blue which stains cartilage acidic mucopolysaccharides and glycosaminoglycans (Fig. 2D). Thus, as it is shown in Fig. 2, the hBM-MSCs that we injected in mice displayed their *in vitro* mesenchymal trilineage differentiation capacity as the ISCT requires [17].

3.3 General monitoring of mice and body weight after transplant

After intrathecal injection, mice were tracked for 24 h or 4 months under GLP conditions. During this time, neither adverse clinical or behavioral symptoms, nor mortality were observed in the control and experimental groups. No significant differences in mean daily water or food consumption were observed between both groups in the experimental period.

Body weight in mice males 9 weeks old (initial weight) was measured before the surgery, and was monitored for 24 h, 15 days, 30 days, 2 and 4 months (Fig. 3). There are no statistical significant differences in the body weight between sham and experimental animals and all of them increased their weight within normal parameters. The initial mean values, before MSCs infusion, from both groups were 21 ± 1.1 grams. One day after the transplant (9 weeks old) the weight was 21.8 ± 1.3 grams; 15 days (11 weeks old) 26.5 ± 1.0 grams; 30 days (13 weeks old) 28.2 ± 1.2 grams; 2 months (17 weeks old) 28.2 ± 1.7 grams and 4 months after the transplant (25 weeks old) 29.5 ± 1.9 grams.

3.4 Clinical hematology and plasma biochemistry: toxicity study

For the hematologic study, we analyzed 3 sham (2 male and 1 female) and 6 transplanted mice (4 male and 2 female) at 24 h post-infusion; and 2 sham (2 male; blood from female was not enough for proper measure) and 5 experimental animals (4 male and 1 female; not enough blood from one female) at 4 months post-infusion. Some previous studies have shown that hematological data from male and female mice are very similar [29, 30]. In our study a few items differ somehow but they were inside the range of the Envigo data guideline (between 6 and 8 weeks). Therefore, in this work we present the averages of each variable for both sexes at 24 h and 4 months (Table 1).

We did not found any statistical difference in hematological values between sham and experimental groups, neither at 24 h nor at 4 months after the transplant (Table 1). However, there were some statistically significant differences in the transplanted animals in MCV (55.30 ± 1.12 fl vs. 52.80 ± 0.57 fl), MCH (15.70 ± 0.10 pg vs. 14.60 ± 0.28 pg) and monocyte count ($0.03 \pm 0.01 \times 10^3/\mu\text{l}$ vs. $0.01 \pm 0.01 \times 10^3/\mu\text{l}$) parameters, being higher in those animals at 24 h versus at 4 months after cell infusion (Table 1). Despite the fact that MCV, MCH and monocytes count changes were statistically significant, the magnitudes of change were inside the normal range.

Regarding the plasma biochemistry values, Table 2 shows the results only from males and cases marked with an asterisk only show one value, due to the limitations in the volume of some mice blood and/or hemolysis. Comparing the data from transplanted animals at 24 h and at 4 months, albumin was significantly higher at 4 months (3.4 ± 0.2 g/dL vs. 4.0 ± 0.2 g/dL; $p < 0,05$), but as in

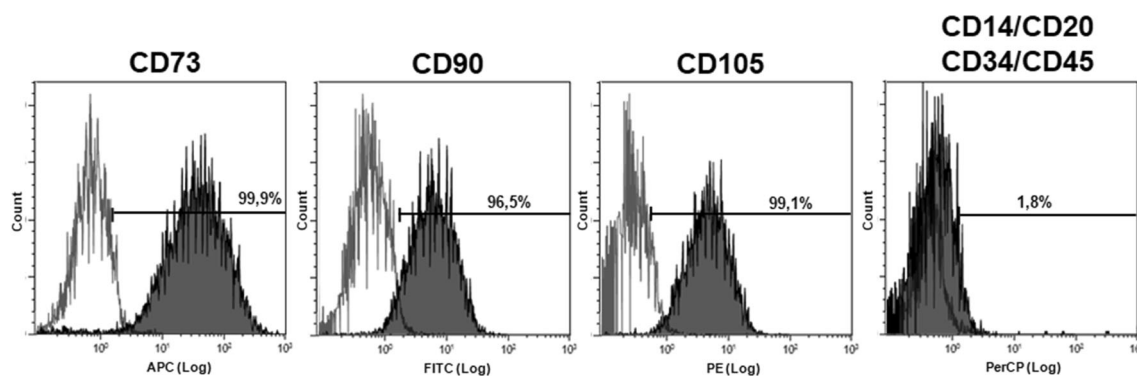


Fig. 1 Cell surface phenotype characterization of human bone marrow-derived mesenchymal stromal cells (hBM-MSCs) by flow cytometry. The histograms show a high expression of the MSCs typical markers CD73, CD90 and CD105, and lack expression of hematopoietic markers such as CD14, CD20, CD34 and CD45. Y-axis

represents cell count. X-axis represents fluorescence intensities in log scale of the fluorochromes allophycocyanin (APC), fluorescein isothiocyanate (FITC), phycoerythrin (PE) and peridinin chlorophyll-protein complex (PerCP), respectively. Numbers inside histograms show percentages of positive cells for each marker

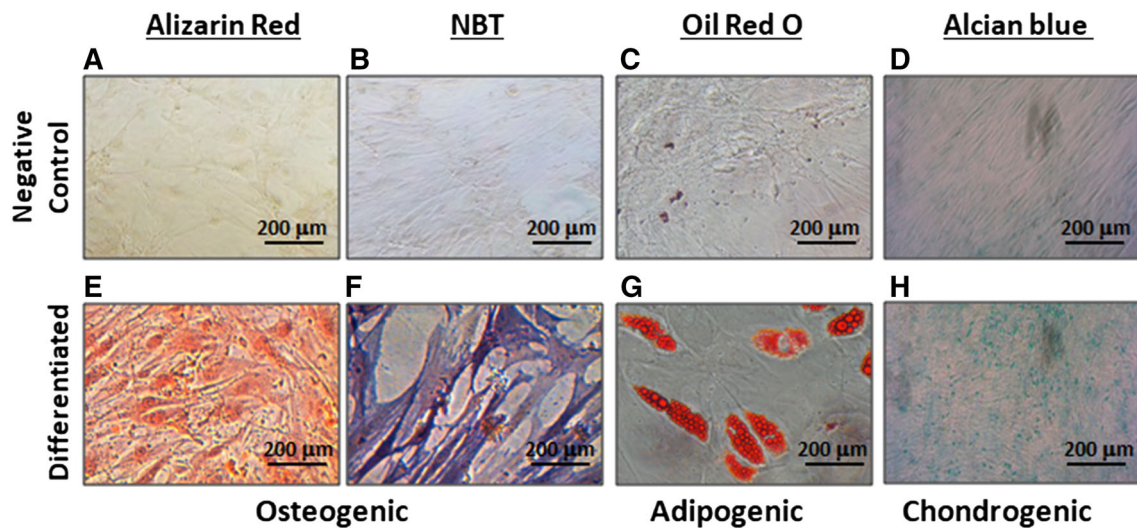


Fig. 2 *In vitro* multilineage differentiation of hBM-MSCs. Osteogenic differentiation was confirmed by the staining of calcium deposition with Alizarin Red (E) and by alkaline phosphatase activity using BCIP-NBT substrate, and visualizing the cells blue-violet (F). Adipogenic differentiation was detected by cytoplasmic oil droplet

accumulation with Oil Red O staining (G) and chondrogenic differentiation was confirmed by the staining of mucopolysaccharides and glycosaminoglycans with Alcian blue staining (H). Undifferentiated control cultures of osteogenic, adipogenic and chondrogenic are shown (A–D)

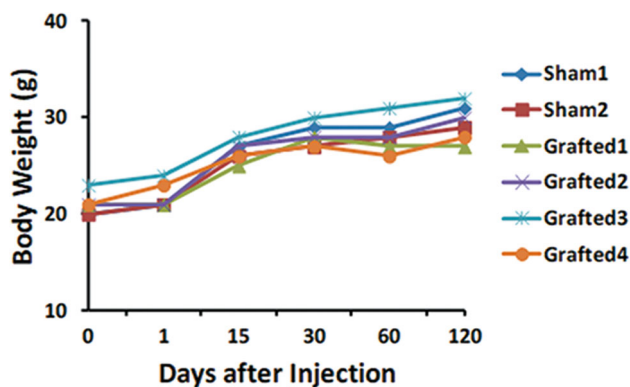


Fig. 3 Body weight changes of sham and experimental male NOD/SCID mice after transplant. The initial weight was measured at 9 weeks old before the transplant (21 ± 1.1 g), and after it: at 1 day (21.8 ± 1.3 g), 15 days (26.5 ± 1.0 g), 30 days (28.2 ± 1.2 g), 60 days (28.2 ± 1.7 g) and 4 months (29.5 ± 1.9 g). The values are inside the normal range. Data are expressed as the mean \pm SD

the hematology data, the magnitudes of change were between the normal ranges.

3.5 Global study of biodistribution of transplanted hBM-MSCs by qPCR

For this purpose, 12 experimental animals ($n = 4$ females; $n = 8$ males) were injected intrathecally with 3×10^5 cells in $5 \mu\text{l}$ of DMEM, whereas 6 control animals ($n = 2$ females; $n = 4$ males) received an intrathecal injection with DMEM alone. Twenty-four hours after the administration, blood samples for biochemical and hematology analysis

were drawn from 6 experimental animals (4 males and 2 females) and 3 control animals (2 males and 1 female). Thereafter the animals were perfused and 9 vital organs (heart, gonads, liver, cerebellum, spleen, lung, spinal cord, brain and kidney) were harvested. Four months after the transplant, this protocol was repeated and those organs were obtained from same number of males and females animals of the experimental and control groups. To analyze whether hBM-MSCs remained in the injection site or migrated to the other tissues, we examined all the collected organs.

Accordingly, gDNA was extracted as a pool from each tissue, and qPCR was run with primers for human β -actin and $\beta 2\text{M}$ gene fragments, and for mouse GAPDH. We obtained GAPDH mouse fragment amplification in all the organs from all the animals (data not shown), indicating that gDNA extraction was performed correctly, that the DNA presented a good purity and confirming that the qPCR reaction had run perfectly. In addition, we concluded that the presence of hMSCs in the analyzed tissue was positive only when both human amplicons β -actin and $\beta 2\text{M}$ were present in the sample. We included a standard curve in each experiment with mouse and/or human gDNA with five dilutions points, which informed us about amplification efficiency (Fig. 4).

Moreover, melting curves were added at the end of each reaction to discriminate a possible unspecific amplification (Fig. 5), which was observed in no case.

We showed that the fragments of human β -actin and $\beta 2\text{M}$ were not amplified in the samples from gonads, liver,

Table 1 Hematological data for transplanted NOD/SCI mice (male and female)

Parameters	24 h		4 months	
	Sham (n = 3)	Engrafted (n = 6)	Sham (n = 2)	Engrafted (n = 5)
RBC ($10^6/\mu\text{l}$)	9.0 ± 0.2	8.6 ± 0.3	7.1 ± 1.8	7.9 ± 1.90
HGB (g/dL)	14.2 ± 0.3	13.4 ± 0.6	10.4 ± 2.5	11.5 ± 2.5
HCT (%)	50.5 ± 1.4	48.0 ± 2.2	36.9 ± 10.5	41.9 ± 9.4
MCV (fl)	55.8 ± 0.6	55.3 ± 1.1*	51.5 ± 1.0	52.8 ± 0.5
MCH (pg)	15.7 ± 0.1	15.5 ± 0.2*	14.5 ± 0.4	14.6 ± 0.2
MCHC (g/dL)	28.1 ± 0.2	28.1 ± 0.4	28.2 ± 1.1	27.6 ± 0.2
Platelet ($10^3/\mu\text{l}$)	856.6 ± 2.8	810.3 ± 187.2	549.5 ± 321.7	710.6 ± 159.1
MPV (fl)	6.7 ± 0.1	6.7 ± 0.1	6.5 ± 0.2	6.9 ± 0.4
WBC ($10^3/\mu\text{l}$)	1.3 ± 0.5	1.0 ± 0.2	0.9 ± 0.5	0.7 ± 0.3
Neutrophils ($10^3/\mu\text{l}$)	0.4 ± 0.3	0.3 ± 0.1	0.3 ± 0.1	0.3 ± 0.1
Lymphocytes ($10^3/\mu\text{l}$)	0.8 ± 0.2	0.6 ± 0.2	0.6 ± 0.3	0.4 ± 0.2
Monocytes ($10^3/\mu\text{l}$)	0.04 ± 0.04	0.03 ± 0.01*	0.02 ± 0.01	0.01 ± 0.01
Eosinophils ($10^3/\mu\text{l}$)	0.03 ± 0.04	0.02 ± 0.04	0.00 ± 0.01	0.01 ± 0.00
Basophils ($10^3/\mu\text{l}$)	0.01 ± 0.01	0.01 ± 0.01	0.01 ± 0.00	0.00 ± 0.01

NOD/SCI mice were injected with DMEM alone (sham) or with hBM-MSCs (engrafted). The values represent mean ± SD, 24 h or 4 months after DMEM or hBM-MSCs transplantation

*Significantly different from sham at 4 months ($p < 0.05$)

Table 2 Biochemistry data for transplanted NOD/SCI mice (male)

Parameters	24 h		4 months	
	Sham (n = 2)	Engrafted (n = 4)	Sham (n = 2)	Engrafted (n = 4)
Glucose (mg/dL)	186.0 ± 0.0 ^a	190.7 ± 42.8	207.5 ± 9.2	199.7 ± 17.2
Urea (mg/dL)	37.0 ± 0.0 ^a	36.5 ± 5.0	Deficient	35.3 ± 2.1
TP (g/dL)	4.9 ± 0.1	4.8 ± 0.2	Deficient	5.0 ± 0.0 ^a
Albumin (g/dL)	3.4 ± 0.2	3.4 ± 0.2*	3.9 ± 0.0 ^a	4.0 ± 0.2
TB (mg/dL)	0.08 ± 0.0	0.1 ± 0.0	0.1 ± 0.0 ^a	0.1 ± 0.0
Na (mEq/L)	149.5 ± 4.9	147.5 ± 5.1	150.0 ± 0.0	148.8 ± 1.3
K (mEq/L)	32.7 ± 4.5	29.2 ± 4.1	26.8 ± 4.2	24.0 ± 2.8
Cl (mEq/L)	101.0 ± 4.2	98.8 ± 4.6	101.0 ± 2.8	102.3 ± 1.5
Triglyceride (mg/dL)	122.0 ± 25.5	107.0 ± 17.8	Deficient	96.0 ± 0.0 ^a
TC (mg/dL)	54.0 ± 0.0 ^a	107.0 ± 7.1	Deficient	97.0 ± 0.0 ^a
AST (U/L)	106.0 ± 0.0 ^a	73.0 ± 0.0 ^a	74.5 ± 23.3	67.0 ± 5.0
ALT (U/L)	21.5 ± 3.5	21.0 ± 4.2	18.0 ± 0.0 ^a	19.3 ± 3.4

NOD/SCI mice were injected with DMEM alone (sham) or with hBM-MSCs (engrafted). The values represent mean ± SD, 24 h or 4 months after DMEM or hBM-MSCs transplantation

^aNot enough plasma. It is shown data from only one mouse

*Significantly different from sham at 4 months ($p < 0.005$)

spleen, lungs, and kidneys from any transplanted animals of both sexes. However, we detected hDNA in the spinal cord on the site of administration in 4/6 animals (2 male and 2 female) 24 h after the transplant; we also detected the presence of hDNA in the heart of one of them (male). Four months after the transplant (n = 6), we found hDNA

amplification in 3 hearts of 3 male, and also in the brain from one of them, but we did not find hDNA amplification in any female organ. In all the control animals (n = 6) in which we injected DMEM alone, we did not detect β -actin or β 2M amplification translating, as expected, the presence of no human cells.

3.6 Histopathological study after 24 h or 4 months from hBM-MSCs transplant

Histological analysis of all the organs was performed by cresyl-violet staining. The results showed that all the animals injected with hBM-MSCs or DMEM alone did not develop any tumor, and no abnormalities or tissue damage were found (Fig. 6).

4 Discussion

Despite the efforts of multiple clinical trials, FRDA remains an incurable disease and there are few therapeutic options which are not able to attenuate its progressive neurodegeneration [8]. Cell therapy with MSCs have been demonstrated to be feasible, very safe and with some efficacy in a variety of human diseases, with an immune or inflammatory pathogenesis as well as in neurodegenerative disorders [31–33].

In our current study, we have developed an accurate analysis of cell biodistribution and potential systemic effects of intrathecal administration of 3×10^5 hBM-MSCs from human healthy donors into the cerebrospinal fluid of immunosuppressed NOD/SCID mice. We demonstrated that these grafts did not produce any toxicity, motor alterations or abnormal behaviour during the experimental time as compared to the control group. The type of

immunosuppressed animals used in this work allowed us to inject human cells without rejection. Preceding experiments in our lab optimized 3×10^5 MSCs as an appropriate number of cells to be injected in mice [26] although the dose of cells may change according to the site of transplant and tissues [20, 34].

Previous works using superoxide dismutase 1 (SOD1) rat model of ALS showed that the combined injection of intraspinal and intravenous MSCs in the animals determines improving general conditions [35], but also a significantly prolonged lifespan, higher motor activity and increased motorneuron survival when the injection was only intrathecal [36]. Intrathecal administration also presents important advantages over intraspinal injection, since it reduces the risk of neurological damage. But, importantly, this administration route bypasses the blood–brain barrier and MSCs can migrate more easily to the damaged tissues in the central nervous system without being trapped in lungs. When the stromal cells are administered intravenously the majority of them get lost in the lung microvasculature, and after crossing the endothelial vessels, very few reach the damaged tissues [37, 38]. To achieve the goal in cell therapy is very important to study the best route of administration of the cell medicinal product. Although precise and disease-selective preclinical data using human MSCs and MSCs-derived neurons in animal models are lacking, various cell therapy trials using the intrathecal route, have not detected any adverse effects

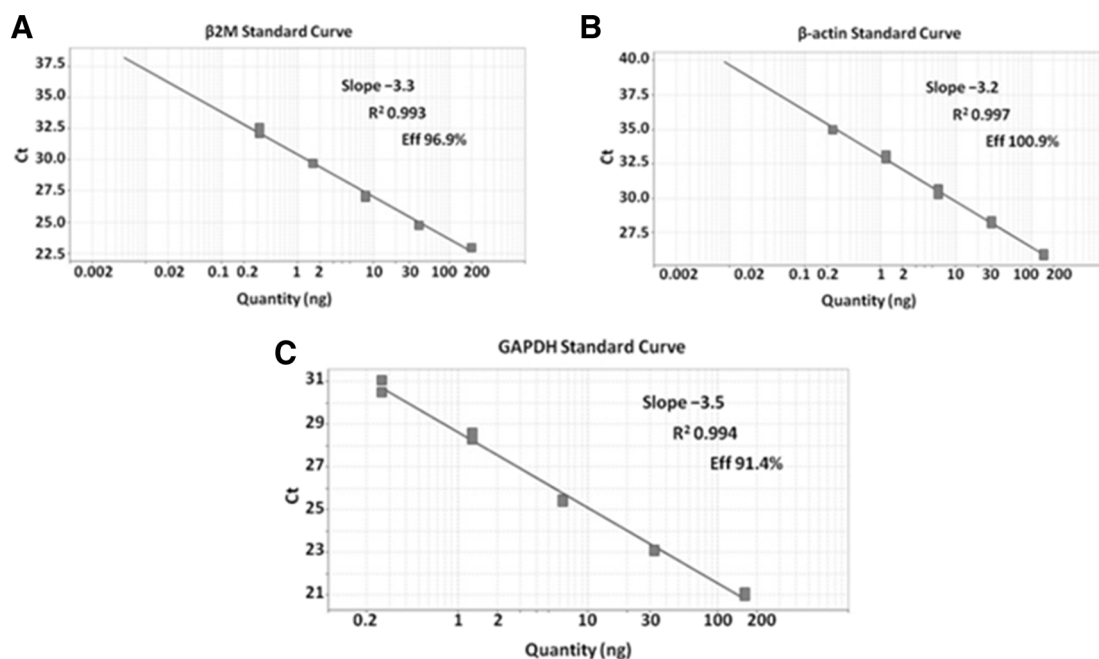


Fig. 4 Representative standard curves of **A** human β 2-microglobulin, **B** human β -actin, and **C** mouse GAPDH. Y-axis indicates the threshold cycle (Ct) values; that is the intersection between an

amplification curve and a threshold line. X-axis indicates the \log_{10} of human or mouse DNA quantity in nanograms (ng)

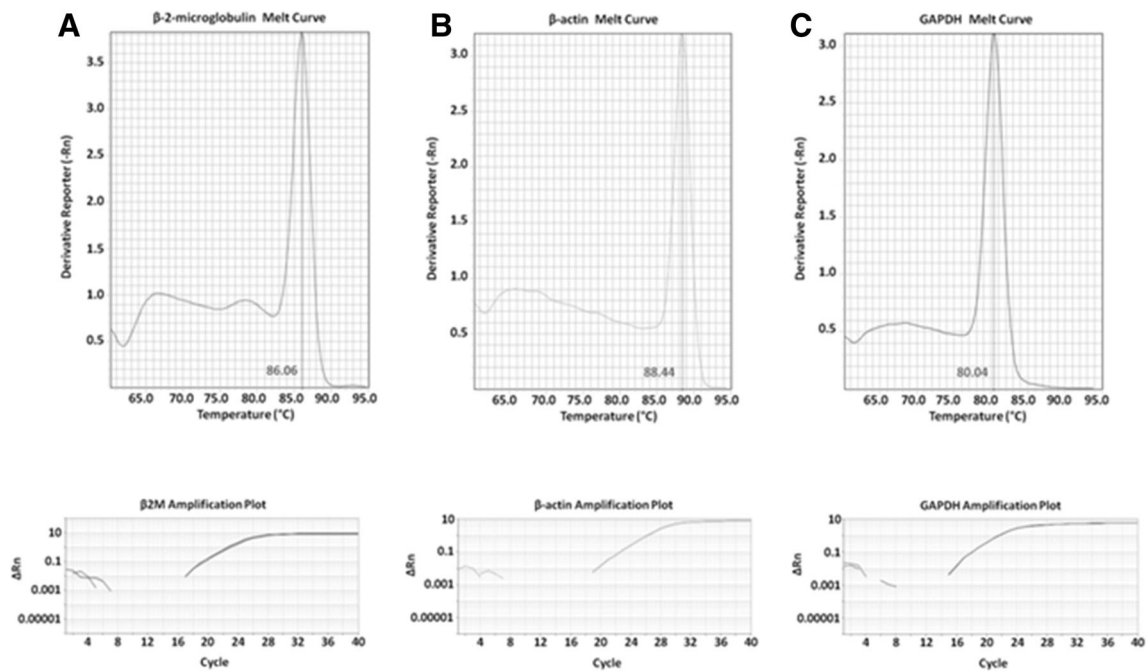


Fig. 5 Representative melting curves of the amplified fragments genes and control gDNAs amplification plots. **A** β 2-microglobulin melting curve with $T_m = 86 \pm 0.5$ °C and amplification in human

gDNA. **B** β -actin melting curve with $T_m = 88.5 \pm 0.5$ °C and amplification in human gDNA. **C** GAPDH melting curve with $T_m = 80 \pm 0.5$ °C and amplification in mouse gDNA

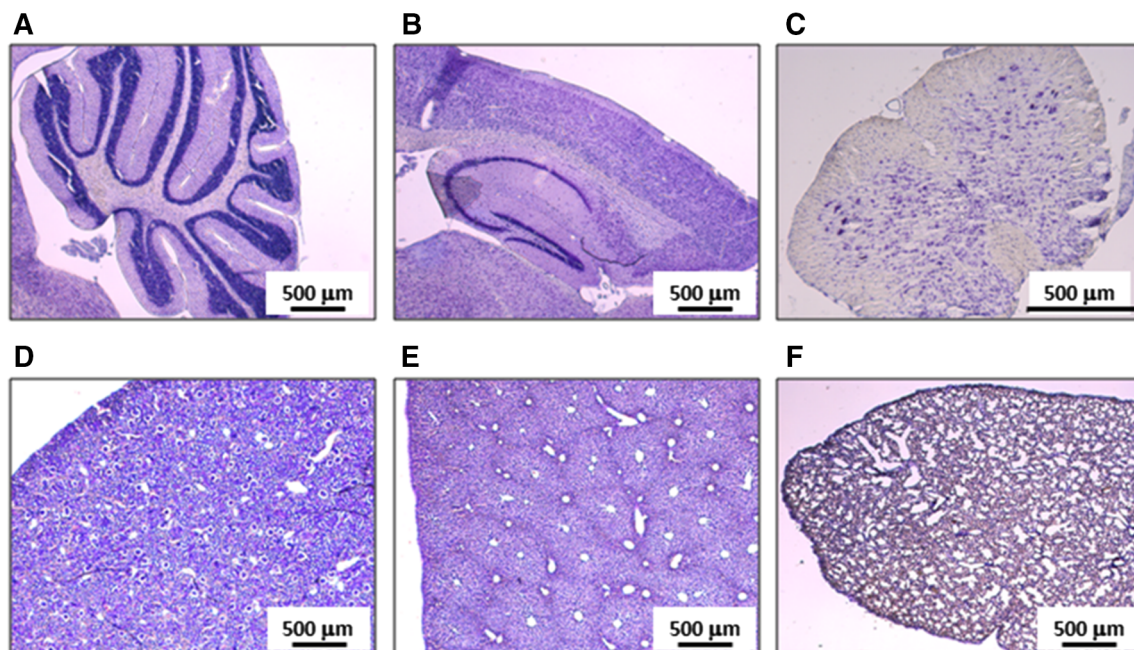


Fig. 6 Tumorigenic analysis of hBM-MSCs injected in NUD/SCID mice. **A** Cerebellum, **B** brain, **C** spinal cord, **D** kidney, **E** liver and **F** lung. In all the analysed tissues, there was no sign of tumour presence and preserved normal histological features

showing that this infusion route is safe [39–41]. In addition there was an increase in regulatory T cell levels [42, 43], and different grades of neuroprotection [11, 14, 15, 44, 45].

Concerning the observed changes in male mice body weight during the experimental period, they were between normal values and the range that Envigo describes in the

growth data, as guideline for NOD.CB17-Prkdc^{scid}/NCRHsd animals; there are no statistically significant differences in body weight between sham and transplanted animals.

On the other hand, the hematological and plasma biochemical data confirmed both the absence of circulating human cells and toxic values in the measured levels. Regarding the small statistically significant changes in MCV, MCH, monocytes count and albumin that we observed in the data between transplanted animals at 24 h versus 4 months, they were inside the normal values presented by the hematologic and clinical chemistry from Envigo. We also obtained normal results in the biochemistry data, but with the limitation that we included only males and in some items only one mouse (marked by an asterisk), because some samples were hemolyzed or with insufficient plasma to obtain measurable results in the analyzer. Accordingly with the normal data obtained in blood parameters, the animals did not present any toxicity and remarkably the histology of all the organs obtained from the 18 animals in this study, showed normal tissue histological appearance with no tumor occurrence.

Our group among others has demonstrated that the qPCR is a sensitive and effective method to quantify and detect small amounts of hDNA in heterogeneous cells populations of tissues from mice engrafted with hMSCs [1, 34, 46]. That is, with this technology we can demonstrate the presence/absence and biodistribution of human cells in mouse tissues with high precision. The use of suitable controls in each plate are determinant to prove whether the amplification reaction has run properly, the quality of the DNA extracted from every tissue is adequate and if there is no contamination in the negative control (no-template control). All the controls in our study amplified when it corresponded: human DNA control sample only amplified when β -actin or β 2M primers were in the master mix reaction, mouse DNA control sample only when GAPDH primers were present and no-template control did not amplify in any plate. On the other hand, the melting curves that we obtained, assured us that the fragments that we amplified were exactly those that we wanted to amplify within the chosen genes (β -actin, β 2M and GAPDH) and not others. All this methodology and the use of fragments from two genes for the detection of human cells, adds security to avoid possible false positives in mice tissues.

With all this, 24 h after the transplant we detected gDNA from human cells in 5/6 spinal cords, suggesting that by this time the infused hBM-MSCs already reach into the spinal cord lepto-meninges in NOD/SCID mice. These results are in agreement with our previous work in wild-type non-FRDA mice where the transplanted BM-MSCs remained in the subarachnoid space at the injected area of the spinal cords until 14 days, while in the FRDA mice

(YG8) they also migrated into the neurodegenerated DRGs, which improved mice behavior tests, decreased neuronal apoptosis and increased glial markers and frataxin expression [14]. That is, MSCs migrate to the injured tissues but, if there is no damage, they remain in the injection site.

Regarding data obtained 4 months after the transplant, we did not detect cells in the spinal cord of any mouse. We did not detect hDNA in any female, but we observed hDNA in the brain of one of these male animals. MSCs injected into the subarachnoid space may arrive to the ventricular system through the cerebrospinal fluid, but most of them are circulating temporarily in this fluid [45, 47]. At this time, we did not detect human cells in other organs. The local distribution of grafted MSCs is consistent with a previous study in which BM-MSCs from green fluorescent protein-positive (GFP⁺) rats were infused intrathecally in healthy rats, and at 14 days they were not observed in brain, spinal cord, liver, spleen or lungs [36]. In other works hDNA was detected at 3 months post-infusion in the thigh and calf injection sites, while it was not detected in heart, lungs, brain, liver, kidneys or spleen [34]. However, using the intra-articular route of administration, MSCs remained during at least 3 months in the joint, but also at some points in time, in the heart, spleen, intestine, brain, blood, or testis [30].

MSCs migrate in the blood and immunosuppressed NOD/SCID mice are prone to myocardium and/or pericardium infections, conditions that might attract migration of infused hBM-MSCs. In this way, it could be possible by this migration that we detected human cells in the hearts of 1/6 treated mice at 24 h and in 3/6 mice at 4 months. Yet, in wild type rats after 14 days of the intrathecal MSCs infusion above the base of the skull, no hBM-MSCs were observed in the spinal cord, brain, lungs, spleen, or liver. But an identical infusion of BM-MSCs in SOD1 rats after 14 days, rescued the perineural nets structure around spinal motoneurons and presented a better survival, proving that even though MSCs cannot be detected, they perform their neuroprotection and anti-apoptotic effect in the damaged tissues [36]. On the other hand, our group has shown that MSCs may also have an effect in distant areas related to the transplant site. In a murine model of motoneuron degeneration, hBM-MSCs were transplanted by intramuscular injection in the hindlimb. Four weeks after the infusion, the cells remained between the basement membrane and the muscle fibers, but we observed an increase in the number of motoneurons that innervate the treated muscle, and in the survival rate of spinal cord motoneurons by axonal-guided retrograde neurotrophism [20]. Furthermore, in a clinical study with a magnetic resonance spectroscopy, after the injection of BM-MSCs at the spinal cord in ALS patients,

we show a distant beneficial effect in the precentral gyri in the brain [48].

Cell therapy with MSCs might be a new approach to change positively the natural evolution in Friedreich's Ataxia, as in other neurodegenerative diseases. MSCs home into injured areas, which are swollen, hypoxic, apoptotic and under oxidative stress, and by displaying its neurotrophic and paracrine activity through neurotrophic factors, cytokines and chemokines, modulate positively the local immune system, reduce apoptosis and free radicals levels, and increase the motoneurons survival [33]. In our lab, we have previously demonstrated that bone marrow stromal cells are capable of protecting neurons in demyelinating, sensory neurons degenerating, cerebellar ataxia and Friedreich's ataxia animal models [14, 24, 26, 49–51].

New therapeutic approaches are critically needed in FRDA patients, and the intrathecal infusion of MSCs might be one of them. The transplantation study presented here, using the immunocompromised NOD/SCID mouse model, with data on biodistribution, toxicology and tumorigenicity represent the required preclinical evaluations necessary to develop a clinical trial with FRDA patients.

Our preclinical study demonstrates that the intrathecal infusion of hBM-MSCs in immunosuppressed mice is feasible and safe. In addition to specifically target the neurodegenerative niche of DRG, it does not produce acute or chronic toxicity evaluated by clinical observation, analytical parameters and tissue histologic examination. It does not produce changes in general behaviour and there were no unexpected deaths or tumor formation. This preclinical study may pave the way to perform clinical human proof of concept of the safety and efficacy of MSCs therapy in patients with Friedreich's Ataxia.

Acknowledgements The authors acknowledge Dra. Carmen Algueró for assistant with flow cytometry, Dr. Tornel-Osorio (Hospital Clínico Universitario Virgen de la Arrixaca) for assistant with the hematology and biochemistry analysis and Dra. Antón-García (Genomic Lab, IMIB-Arrixaca) for technical assistance. This work was supported by the Fundación Mutua Madrileña (API62842016), Asociación Granadina de Ataxia de Friederich (ASOGAF), Instituto de Salud Carlos III (ISCIII) Spanish Net of Cell Therapy (TerCel), RETICS subprogram of the I + D + I 2013–2016 Spanish National Plan, Projects “RD12/0019/0001”, “RD12/0019/0023”, “RD16/0011/0001” and “RD16/0011/0010” funded by ISCIII and co-founded by European Regional Development Funds.

Compliance with ethical standards

Conflict of interest The authors declare that they have no conflict of interest.

Ethical statement The use of human bone marrow cells was in accordance with the guidelines and regulations of the Ethics Committee of the Hospital Clínico Universitario Virgen de la Arrixaca (Murcia, Spain). All of the donors provided written informed consent

prior to participation in this study. The procedures performed in this work involving animals were approved by the Ethical Committee on Animal Experimentation at University of Murcia (220/2016). All the experimental procedures involving animals were conducted in accordance with the Institutional Animal care guidelines of Murcia University.

References

1. Reyes B, Coca MI, Codinach M, López-Lucas MD, Del Mazo-Barbara A, Caminal M, et al. Assessment of biodistribution using mesenchymal stromal cells: algorithm for study design and challenges in detection methodologies. *Cytotherapy*. 2017;19:1060–9.
2. Campuzano V, Montermini L, Moltò MD, Pianese L, Cossée M, Cavalcanti F, et al. Friedreich's ataxia: autosomal recessive disease caused by an intronic GAA triplet repeat expansion. *Science*. 1996;271:1423–7.
3. Punga T, Bühler M. Long intronic GAA repeats causing Friedreich ataxia impede transcription elongation. *EMBO Mol Med*. 2010;2:120–9.
4. Schulz JB, Boesch S, Bürk K, Dürr A, Giunti P, Mariotti C, et al. Diagnosis and treatment of Friedreich ataxia: a European perspective. *Nat Rev Neurol*. 2009;5:222–34.
5. Koeppen AH. Friedreich's ataxia: pathology, pathogenesis, and molecular genetics. *J Neurol Sci*. 2011;303:1–12.
6. Pousset F, Legrand L, Monin ML, Ewencyk C, Charles P, Komajda M, et al. A 22-year follow-up study of long-term cardiac outcome and predictors of survival in Friedreich ataxia. *JAMA Neurol*. 2015;72:1334–41.
7. Delatycki MB, Corben LA. Clinical features of Friedreich ataxia. *J Child Neurol*. 2012;27:1133–7.
8. Marmolino D. Friedreich's ataxia: past, present and future. *Brain Res Rev*. 2011;67:311–30.
9. Koeppen AH, Ramirez RL, Becker AB, Mazurkiewicz JE. Dorsal root ganglia in Friedreich ataxia: satellite cell proliferation and inflammation. *Acta Neuropathol Commun*. 2016;4:46.
10. Long A, Napierala JS, Polak U, Hauser L, Koeppen AH, Lynch DR, et al. Somatic instability of the expanded GAA repeats in Friedreich's ataxia. *PLoS One*. 2017;12:e0189990.
11. Moraleda JM, Blanquer M, Bleda P, Iniesta P, Ruiz F, Bonilla S, et al. Adult stem cell therapy: dream or reality? *Transpl Immunol*. 2006;17:74–7.
12. Blanquer M, Moraleda JM, Iniesta F, Gómez-Espuch J, Meca-Lallana J, Villaverde R, et al. Neurotrophic bone marrow cellular nests prevent spinal motoneuron degeneration in amyotrophic lateral sclerosis patients: a pilot safety study. *Stem Cells*. 2012;30:1277–85.
13. Bueno C, Ramirez C, Rodríguez-Lozano FJ, Tabarés-Seisdedos R, Rodenas M, Moraleda JM, et al. Human adult periodontal ligament-derived cells integrate and differentiate after implantation into the adult mammalian brain. *Cell Transplant*. 2013;22:2017–28.
14. Jones J, Estirado A, Redondo C, Pacheco-Torres J, Sirerol-Piquer MS, Garcia-Verdugo JM, et al. Mesenchymal stem cells improve motor functions and decrease neurodegeneration in ataxic mice. *Mol Ther*. 2015;23:130–8.
15. Ruiz-López FJ, Blanquer M. Autologous bone marrow mononuclear cells as neuroprotective treatment of amyotrophic lateral sclerosis. *Neural Regen Res*. 2016;11:568–9.
16. Rodríguez-Lozano FJ, Bueno C, Insausti CL, Meseguer L, Ramírez MC, Blanquer M, et al. Mesenchymal stem cells derived from dental tissues. *Int Endod J*. 2011;44:800–6.

17. Dominici M, Le Blanc K, Mueller I, Slaper-Cortenbach I, Marini F, Krause D, et al. Minimal criteria for defining multipotent mesenchymal stromal cells. The international society for cellular therapy position statement. *Cytotherapy*. 2006;8:315–7.
18. Wang Y, Chen X, Cao W, Shi Y. Plasticity of mesenchymal stem cells in immunomodulation: pathological and therapeutic implications. *Nat Immunol*. 2014;15:1009–16.
19. Mazzini L, Fagioli F, Boccaletti R, Mareschi K, Oliveri G, Olivieri C, et al. Stem cell therapy in amyotrophic lateral sclerosis: a methodological approach in humans. *Amyotroph Lateral Scler Other Motor Neuron Disord*. 2003;4:158–61.
20. Pastor D, Viso-León MC, Botella-López A, Jaramillo-Merchan J, Moraleda JM, Jones J, et al. Bone marrow transplantation in hindlimb muscles of motoneuron degenerative mice reduces neuronal death and improves motor function. *Stem Cells Dev*. 2013;22:1633–44.
21. Quesada MP, Jones J, Rodríguez-Lozano FJ, Moraleda JM, Martínez S. Novel aberrant genetic and epigenetic events in Friedreich's ataxia. *Exp Cell Res*. 2015;335:51–61.
22. Jones J, Estirado A, Redondo C, Bueno C, Martínez S. Human adipose stem cell-conditioned medium increases survival of Friedreich's ataxia cells submitted to oxidative stress. *Stem Cells Dev*. 2012;21:2817–26.
23. Kemp K, Mallam E, Hares K, Witherick J, Scolding N, Wilkins A. Mesenchymal stem cells restore frataxin expression and increase hydrogen peroxide scavenging enzymes in Friedreich ataxia fibroblasts. *PLoS One*. 2011;6:e26098.
24. Jones J, Estirado A, Redondo C, Martínez S. Stem cells from wildtype and Friedreich's ataxia mice present similar neuroprotective properties in dorsal root ganglia cells. *PLoS One*. 2013;8:e62807.
25. Rocca CJ, Goodman SM, Dulin JN, Haquang JH, Gertsman I, Blondelle J, et al. Transplantation of wild-type mouse hematopoietic stem and progenitor cells ameliorates deficits in a mouse model of Friedreich's ataxia. *Sci Transl Med*. 2017;9:eaaj2347
26. Cabanes C, Bonilla S, Tabares L, Martínez S. Neuroprotective effect of adult hematopoietic stem cells in a mouse model of motoneuron degeneration. *Neurobiol Dis*. 2007;26:408–18.
27. Selvadurai LP, Harding IH, Corben LA, Georgiou-Karistianis N. Cerebral abnormalities in Friedreich ataxia: a review. *Neurosci Biobehav Rev*. 2018;84:394–406.
28. Harris VK, Vyshkina T, Sadiq SA. Clinical safety of intrathecal administration of mesenchymal stromal cell-derived neural progenitors in multiple sclerosis. *Cytotherapy*. 2016;18:1476–82.
29. Choi SA, Yun JW, Joo KM, Lee JY, Kwak PA, Lee YE, et al. Preclinical biosafety evaluation of genetically modified human adipose tissue-derived mesenchymal stem cells for clinical applications to brainstem glioma. *Stem Cells Dev*. 2016;25:897–908.
30. Toupet K, Maumus M, Peyrafitte JA, Bourin P, van Lent PL, Ferreira R, et al. Long-term detection of human adipose-derived mesenchymal stem cells after intraarticular injection in SCID mice. *Arthritis Rheum*. 2013;65:1786–94.
31. Lalu MM, McIntyre L, Pugliese C, Fergusson D, Winston BW, Marshall JC, et al. Safety of cell therapy with mesenchymal stromal cells (SafeCell): a systematic review and meta-analysis of clinical trials. *PLoS One*. 2012;7:e47559.
32. Ullah I, Subbarao RB, Rho GJ. Human mesenchymal stem cells—current trends and future prospective. *Biosci Rep*. 2015;35:e00191
33. Joyce N, Annett G, Wirthlin L, Olson S, Bauer G, Nolte JA. Mesenchymal stem cells for the treatment of neurodegenerative disease. *Regen Med*. 2010;5:933–46.
34. Creane M, Howard L, O'Brien T, Coleman CM. Biodistribution and retention of locally administered human mesenchymal stromal cells: quantitative polymerase chain reaction-based detection of human DNA in murine organs. *Cytotherapy*. 2017;19:384–94.
35. Forostyak S, Jendelova P, Kapcalova M, Arboleda D, Sykova E. Mesenchymal stromal cells prolong the lifespan in a rat model of amyotrophic lateral sclerosis. *Cytotherapy*. 2011;13:1036–46.
36. Forostyak S, Homola A, Tumovcova K, Svitil P, Jendelova P, Sykova E. Intrathecal delivery of mesenchymal stromal cells protects the structure of altered perineuronal nets in SOD1 rats and amends the course of ALS. *Stem Cells*. 2014;32:3163–72.
37. Leibacher J, Henschler R. Biodistribution, migration and homing of systemically applied mesenchymal stem/stromal cells. *Stem Cell Res Ther*. 2016;7:7.
38. François S, Usunier B, Douay L, Benderitter M, Chapel A. Long-term quantitative biodistribution and side effects of human mesenchymal stem cells (hMSCs) engraftment in NOD/SCID mice following irradiation. *Stem Cells Int*. 2014;2014:939275.
39. Harris VK, Stark J, Vyshkina T, Blackshear L, Joo G, Stefanova V, et al. Phase I trial of intrathecal mesenchymal stem cell-derived neural progenitors in progressive multiple sclerosis. *EBioMedicine*. 2018;29:23–30.
40. Santamaría AJ, Benavides FD, DiFede DL, Khan A, Pujol MV, Dietrich WD, et al. Clinical and neurophysiological changes after targeted intrathecal injections of bone marrow stem cells in a C3 tetraplegic subject. *J Neurotrauma*. 2019;36:500–16.
41. Vaquero J, Zurita M, Rico MA, Aguayo C, Bonilla C, Marin E, et al. Intrathecal administration of autologous mesenchymal stromal cells for spinal cord injury: safety and efficacy of the 100/3 guideline. *Cytotherapy*. 2018;20:806–19.
42. Karussis D, Karageorgiou C, Vaknin-Dembinsky A, Gowda-Kurkalli B, Gomori JM, Kassis I, et al. Safety and immunological effects of mesenchymal stem cell transplantation in patients with multiple sclerosis and amyotrophic lateral sclerosis. *Arch Neurol*. 2010;67:1187–94.
43. Petrou P, Gotthelf Y, Argov Z, Gotkine M, Levy YS, Kassis I, et al. Safety and clinical effects of mesenchymal stem cells secreting neurotrophic factor transplantation in patients with amyotrophic lateral sclerosis: results of phase 1/2 and 2a clinical trials. *JAMA Neurol*. 2016;73:337–44.
44. Oh KW, Moon C, Kim HY, Oh SI, Park J, Lee JH, et al. Phase I trial of repeated intrathecal autologous bone marrow-derived mesenchymal stromal cells in amyotrophic lateral sclerosis. *Stem Cells Transl Med*. 2015;4:590–7.
45. Syková E, Rychmach P, Drahorádová I, Konrádová S, Růžicková K, Voříšek I, et al. Transplantation of mesenchymal stromal cells in patients with amyotrophic lateral sclerosis: results of phase I/IIa clinical trial. *Cell Transplant*. 2017;26:647–58.
46. McBride C, Gaupp D, Phinney DG. Quantifying levels of transplanted murine and human mesenchymal stem cells in vivo by real-time PCR. *Cytotherapy*. 2003;5:7–18.
47. Kim H, Kim HY, Choi MR, Hwang S, Nam KH, Kim HC, et al. Dose-dependent efficacy of ALS-human mesenchymal stem cells transplantation into cisterna magna in SOD1-G93A ALS mice. *Neurosci Lett*. 2010;468:190–4.
48. García Santos JM, Inuggi A, Gómez Espuch J, Vázquez C, Inieta F, Blanquer M, et al. Spinal cord infusion of stem cells in amyotrophic lateral sclerosis: magnetic resonance spectroscopy shows metabolite improvement in the precentral gyrus. *Cytotherapy*. 2016;18:785–96.

49. Bonilla S, Silva A, Valdés L, Geijo E, García-Verdugo JM, Martínez S. Functional neural stem cells derived from adult bone marrow. *Neuroscience*. 2005;133:85–95.
50. Pastor D, Viso-León MC, Jones J, Jaramillo-Merchán J, Toledo-Aral JJ, Moraleda JM, et al. Comparative effects between bone marrow and mesenchymal stem cell transplantation in GDNF expression and motor function recovery in a motoneuron degenerative mouse model. *Stem Cell Rev*. 2012;8:445–58.
51. Jones J, Jaramillo-Merchán J, Bueno C, Pastor D, Viso-León M, Martínez S. Mesenchymal stem cells rescue Purkinje cells and improve motor functions in a mouse model of cerebellar ataxia. *Neurobiol Dis*. 2010;40:415–23.

Publisher's Note Springer Nature remains neutral with regard to jurisdictional claims in published maps and institutional affiliations.